Defence Science Journal, Vol. 71, No. 2, March 2021, pp. 231-240, DOI : 10.14429/dsj.71.15772

Performance of a Cantilever Energy Harvester under Harmonic and Random Excitations

K. Manoj[#,@], V. Narayanamurthy[@,*], and S. Korla[#]

[#]*National Institute of Technology, Warangal - 506 004, India*
[@]*DRDO-Research Centre Imarat, Hyderabad - 500 069, India*
[*]*E-mail : v.narayanamurthy@rcilab.in*

ABSTRACT

The technique of harvesting the energy from base structural vibration through a piezoelectric transducer attached at an appropriate location on the vibrating structure is gaining popularity in recent years. Although the amount of energy harvested depends on the type and magnitude of base excitation, the energy harvest under random excitation as compared to equivalent harmonic excitations is not yet well understood and is investigated in this paper through a cantilever energy harvester. Initially, the energy harvested under harmonic excitations is numerically simulated and experimentally validated under increasing base accelerations with different load resistances. Subsequently, the performance of this energy harvester is experimentally studied under random excitations. The results demonstrate that the harvested energy (a) reaches maximum value when the base excitation matches the natural frequency of the harvester, (b) increases with the increase in base accelerations irrespective of the type of excitation, and (c) increases by 2-14 times under random excitations as compared to equivalent harmonic excitations i.e. under same energy input. It is recommended that the energy harvester be used in aerospace structures where random vibration amplitude is higher, to harvest more energy.

Keywords: Vibration energy harvester; Harmonic and random excitations; Numerical simulations; Base acceleration; Power output

1. INTRODUCTION

The aerospace vehicles typically have hundreds to few thousands of sensors at various locations for monitoring various in-flight parameters like strain, temperature, pressure, shock, velocity, acceleration, vibration, etc., on airframe, wings, control systems, engine, landing gear, fuel/oxidiser tanks, etc., for assessing the health of the structure and subsystems. Conventionally, these wired sensors and data acquisition systems suffer from complexities in cable harness, large data sets and measurement points. These limitations led to the development of wireless sensor network systems, in recent years, which demand low-power electricity from batteries located near sensors. But these are again challenged by battery power, duration, cost of battery replacement, etc. Therefore, generating low-power electricity from inevitable base structural vibrations[1–6] using energy harvesters is emerging as an alternate source of power for these applications.

Roundy[1], *et al.* and others[7–16] investigated and evaluated different energy conversion mechanisms leading to optimised designs for piezoelectric, electromagnetic, electrostatic, and tribo-electric transducers. Anton and Sodano[4] showed that the piezoelectric transduction is suitable for vibration energy harvesting due to its high-power density and ease of application of piezoelectric materials. Abdelkefi[17], *et al.* and Liu[18], *et al.* investigated the benefits of matching the natural frequencies of an energy harvester with that of excitation to extract more energy from vibrating structure and proposed that this will be more effective with multiple matched resonant frequencies. Ashraf[19], *et al.* emphasised the design of an energy harvester for low frequency excitation but reported the challenges of large amplitudes, demanding large damping, dropping of average power flowing into the harvester and the requirement of large electromechanical coupling. Nechibvute[20], *et al.* suggested that a series bimorph device can be optimised for power generation when the ratio of the length of the piezoelectric layer to that of the proof mass is 50 %. Yu[21], *et al.* numerically investigated a micro-electro-mechanical system based piezoelectric energy harvester (PEH) and showed improved energy storage efficiency using an autonomous power conditioning circuit, impedance matching, energy storage and voltage regulation. Xu[22] introduced four concepts of PEHs such as 1) cantilever beam PEH, 2) flex-tensional PEH, 3) edge-clamped PEH, and 4) advanced PEH. He discussed their relative performances and recommended flex-tensional PEH for maximum energy harvesting. Tuma[23], *et al*. introduced design methods of natural frequency for double-piezoelectric cantilever beams.

Adhikari, *et al.*[24] studied a non-linear piezo-magneto-elastic energy harvester and demonstrated an increase in the harvested energy for harmonic excitation with slowly varying frequency. Kim[25], *et al.* discussed the vibration analysis of

Received : 29 April 2020, Revised : 04 January 2021
Accepted : 04 January 2021, Online published : 10 March 2021

cantilever-bimorph energy harvester having a proof mass at the tip. Leng[26], *et al.* investigated a tri-stable PEH with two external magnets for studying the response of large-amplitude and broadband voltage. Erturk[27], *et al*. studied different electromechanical models of PEH beams and provided corrections and clarifications in modelling of PEHs. Soliman[28], *et al.* investigated the energy harvesters under wide band excitation. Liu[29], *et al.* discussed the energy harvest from acoustic vibrations adopting an electromechanical Helmholtz resonator. Gibus[30], *et al.* reported an analytical model for optimising the electromechanical coupling of a vibration based energy harvester. Shu[31-33], *et al.* developed analytical expression for power output under steady state operation. Ng[34], *et al.* studied a self-powered piezoelectric sensor, in which a piezoelectric element is used as a power generator from vibration. On the other hand, Renno[35], *et al.* tried to optimise the power by employing resistive and inductive loads. Several researchers[36-38] developed different closed-form solutions for the optimal conditions under deterministic excitations. In many cases, the vibrational energy is non-harmonic or entirely stochastic, with broad frequency content. Very few researchers[39-43] have investigated energy harvesting from random vibrations.

The vibration levels that excite the harvester vary depending upon the application or the base structure on which the harvester is mounted. The vibration can be with single harmonic source, multiple harmonic source, a repeating step / ramp excitation or a random vibration with continuously varying frequencies in a given frequency range. Most existing research were under harmonic excitations either based on theoretical (with simplified assumptions), or experimental with base structure as machineries, bridges and pedestrian pavements. Only few numerical studies based on FEA of these harvesters are reported. Performance of these harvesters under random excitations with continuously varying frequencies and varying accelerations as experienced in aerospace vehicles are not yet well explored and so are their relative assessment with equivalent harmonic excitations.

The research reported in this paper addresses these limitations through a piezoelectric cantilever energy harvester (CEH) as illustrated in Fig. 1, where L is the length, h_s is the substrate thickness, h_p is the piezo-layer thickness and R is the resistive load. The beam resembles a composite structure (of perfectly bonded isotropic) and follows Euler- Bernoulli beam assumptions. Initially, the energy harvested under harmonic excitations is numerically simulated under increasing base accelerations with different load resistances and experimentally validated. Subsequently, the performance of this PEH is experimentally investigated under random excitations and compared with equivalent harmonic excitations. Further, this paper presents the development of the experimental method and procedure to perform these experiments on the energy harvester.

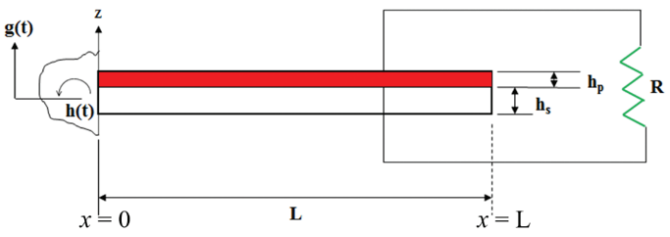

Figure 1. CEH transversely excited by the translation and small rotation at its base.

2. NUMERICAL SIMULATION OF CEH UNDER HARMONIC EXCITATION

The CEH subjected to a harmonic excitation at its base structure is numerically simulated using the FEA code, ANSYS[44]. Initially, the energy harvested under harmonic excitation matching the natural frequency of the CEH is investigated. This is followed by the prediction of its performance under increasing base acceleration levels, typically for three different load resistances.

2.1 Geometry and Material Properties

The CEH consists of a piezoelectric unimorph. The piezo electric substrate used in present study is a semi-crystalline PVDF (Polyvinylidene fluoride), LTD4-28K/L of 40 μm thickness and bonded over an aluminium alloy AA2014 base cantilever beam of dimensions 171x22x2 mm as shown in Fig. 2(a) in which the geometry of the harvesting structure with piezoelectric layer is shown in red colour and aluminium substrate in grey colour. A ϕ6 mm hole is provided at the fixed end of this harvester for clamping with the base exciting structure. The piezoelectric material is bonded to the aluminium substructure by cyanoacrylate adhesive Mbond 200. The actual configuration of the harvester is shown in Fig. 2(b). The properties of PVDF taken from manufacturer's data sheet are given in Table 1 which are used as inputs in FEA simulations.

Table 1. Properties of PVDF substrate

Property	Value	Unit
Density	1780	kg/m^3
Piezoelectric strain constant (d_{31})	23 x 10^{-12}	C/N
Piezoelectric strain constant (d_{33})	-33 x 10^{-12}	C/N
Piezoelectric stress constant (g_{31})	216 x 10^{-3}	Vm/N
Piezoelectric stress constant (g_{33})	-330 x 10^{-3}	Vm/N
Electromechanical coupling factor (k_{31})	12.0%	-
Electromechanical coupling factor (k_t)	14.0%	-
Young's modulus of elasticity (E)	4.0	GPa
Capacitance (C)	11.0	nF

2.2 Model setup for FEA

A simplified geometric model of CEH as shown in Fig. 3(a) is modelled in ANSYS 18.1 Workbench Space claim[44]. The FEA model with piezoelectric material properties is prepared in *PiezoAndMEMS* extension module. This model is made up of three parts a) aluminium alloy base structure, b) piezoelectric material i.e. PVDF, and c) resistor. The PVDF is attached to the aluminium substructure using a bonded connection i.e. a rigid bond behaviour. All three components of CEH are discretised for FEA. Aluminium alloy substructure is discretised by 356 elements and PVDF by 60 elements. Both are discretised by 20 node tetrahedron elements having translational nodal degrees of freedom in x, y and z directions.

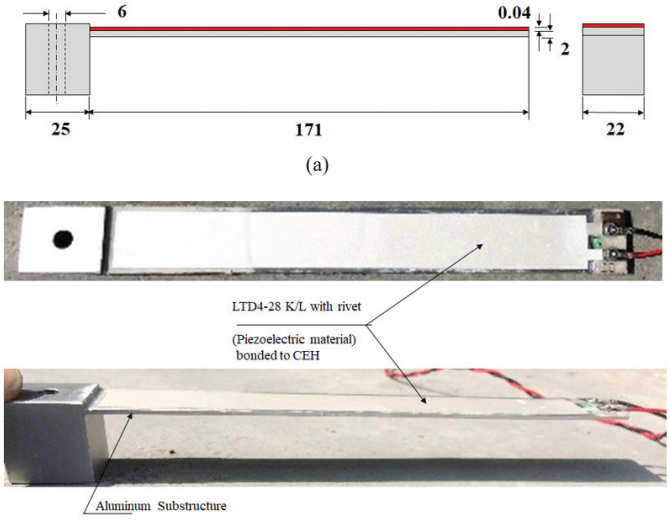

Figure 2. Unimorph cantilever energy harvester: (a) Geometry of cantilever energy harvester (all dimensions in mm) and (b) Physical configuration.

The CIRCU 94 element is chosen to simulate basic linear electric circuit components that can be directly connected to the piezoelectric FEA domain. Since resistor is being used as load, the *keyopt* (1) = 0 with resistance 102 kΩ is chosen. This resistor component is 1-dimensional and discretised with single 1-D element which has two nodes, each node having voltage as the degree of freedom.

The meshed FE model of the CEH with boundary conditions is shown in Fig. 3(b). The material properties for aluminium alloy substructure, piezoelectric material and resistor are assigned for the FEA model as per the values provided in Tables 1 and 2. Polystyrene material available in database[40] is assigned to the resistor with a resistance value of 102 kΩ. The voltage degree of freedom at nodes 1 and 2 of resistor are coupled with the terminals of PVDF.

2.3 Numerical Simulation

Initially, in the first stage, modal analysis was carried out for the CEH considering a damping coefficient of 0.02, as shown in Fig. 3(a-b) and predicted a fundamental natural frequency of 27.5 Hz as shown in Fig. 3(c).

Table 2. Properties of aluminium alloy AA2014 material

Properties	Value
Density (kg/m^3)	2650
Modulus of elasticity (MPa)	70000
Poisson's ratio	0.3

Subsequently, in the second stage, numerical simulations were carried out on CEH subjected to a harmonic base structural excitation at the fixed end with an acceleration level of 9.8 m/s^2 i.e. at 1g with a frequency varying from 10 Hz to 50 Hz under a load resistance of 102 kΩ. The plots for the voltage, current and power generated with respect to the excitation frequency are shown in Fig. 4. It is observed that the energy harvested is maximum when the base excitation matches the CEH's natural frequency. The corresponding maximum voltage, current and power harvested are 0.32 V, 3.15 μA and 1.04 μW, respectively. It can be noted here that although the modal analysis of CEH resulted in 27.5 Hz (as seen in

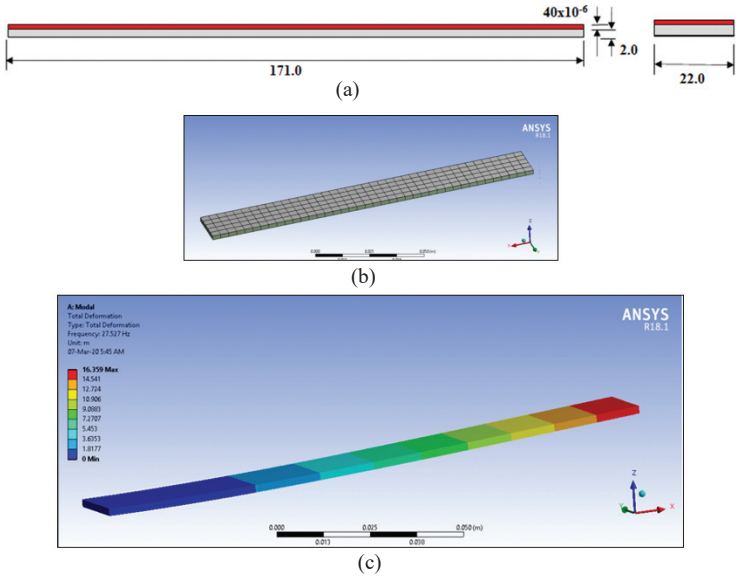

Figure 3. FEA model set up and first mode shape of unimorph cantilever energy harvester: (a) Geometry of FEA model, (b) Discretised FE model with boundary condition (All displacement components $u_x = u_y = u_z = 0$ at left end), and (c) First mode shape (at 27.5 Hz).

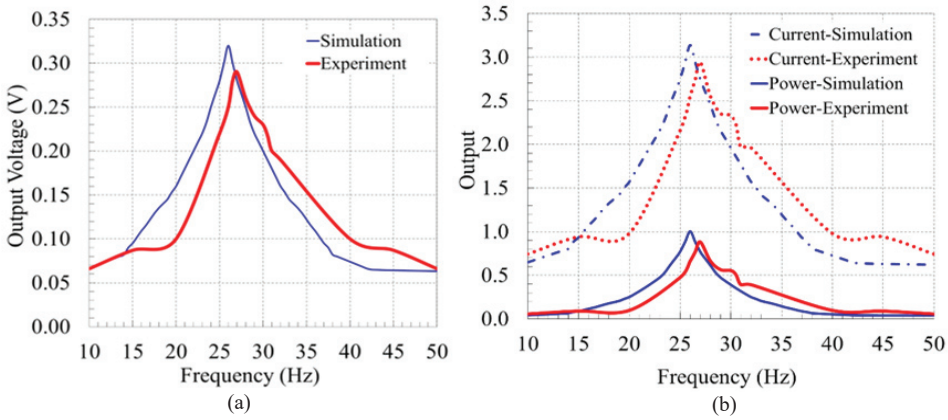

Figure 4. Energy harvested from simulation versus experiment for R=102 kΩ under harmonic excitation, (a) Voltage output and (b) Current (μA) and power output (μW).

Fig. 3c) as the fundamental natural frequency which was also used for exciting the base structure harmonically, the maximum response of voltage, current and power occurred at 26.5 Hz, i.e. 1 Hz before the computed natural frequency. The reduction of 1 Hz in present simulation is due to the inclusion of load resistors which was not considered in the first stage of analysis i.e. modal analysis. As the harvested energy is maximum only at resonant frequencies, it can be concluded based on predicted response that the fundamental frequency of CEH including load resistors is 26.5 Hz only.

In the third stage, the simulations were repeated twice with two more additional resistances of 150 kΩ and 260 kΩ with frequency of excitation varying from 10 Hz to 50 Hz and at 1g acceleration level to understand the performance with increase in load resistances. The predictions reveal that the harvested energy is always maximum when CEH is excited at its natural frequency, irrespective of the magnitude of the load resistance. As the load resistance is increased, the voltage output increases and the current generated decreases. Maximum voltages of 0.32 V, 0.37 V and 0.49 V and maximum currents of 3.15 μA, 2.45 μA, and 1.85 μA were generated, respectively at load resistances of 102 kΩ, 150 kΩ and 260 kΩ as shown in Fig. 5(a-b). On the other hand, as the load resistance is increased, the power generated decreases but the decrease is only marginal or negligible at 150 kΩ and 260 kΩ. The power generated is 1.04 μW at 102 kΩ and it is only 0.93 μW at 150 kΩ and 260 kΩ as shown in Fig. 5(c). This demonstrates that the power generated is almost constant beyond 150 kΩ of load resistance when base is excited with 1g acceleration.

In the fourth stage, further simulations were carried out by exciting the base structure of CEH harmonically at natural frequency and at different acceleration levels varying from 1g to 10g with load resistance as 102 kΩ. This is repeated with two more additional load resistances of 150 kΩ and 260 kΩ to investigate the harvested energy at increasing acceleration levels and increasing load resistances. All excitations were carried out at natural frequency in order to quantify the maximum possible energy output. Figs. 6(a-c) respectively show the plots of maximum voltage, current and power generated by the CEH at three different load resistances with respect to increasing base acceleration. As the load resistance is increased, the voltage output increases and the current and power generated decreases at any given acceleration level but the voltage, current and power generated increases with the increase in base acceleration. It is to be noted that the decrease in power output when load resistances are increased is predominantly visible only at higher acceleration levels as seen in Fig. 6(c). On contrary, this decrease with increase in load resistance beyond 150 kΩ is negligible at 1g level of base acceleration as seen in Fig. 5(c).

The increase in voltage output is from 0.32 V to 1.44 V with increase in base acceleration from 1g to 10g at 102 kΩ of load resistance. The corresponding increase is from 0.37 V to 1.64 V and 0.49 V to 2.5 V, respectively at load resistances of 150 kΩ and 260 kΩ as shown in Fig. 6(a). The increase in current output is from 3.15 μA to 14.2 μA, 2.45 μA to 11.0 μA and 1.85 μA to 7.8μA, respectively at load resistances of 102 kΩ, 150 kΩ and 260 kΩ as shown in Fig. 6(b). The increase in

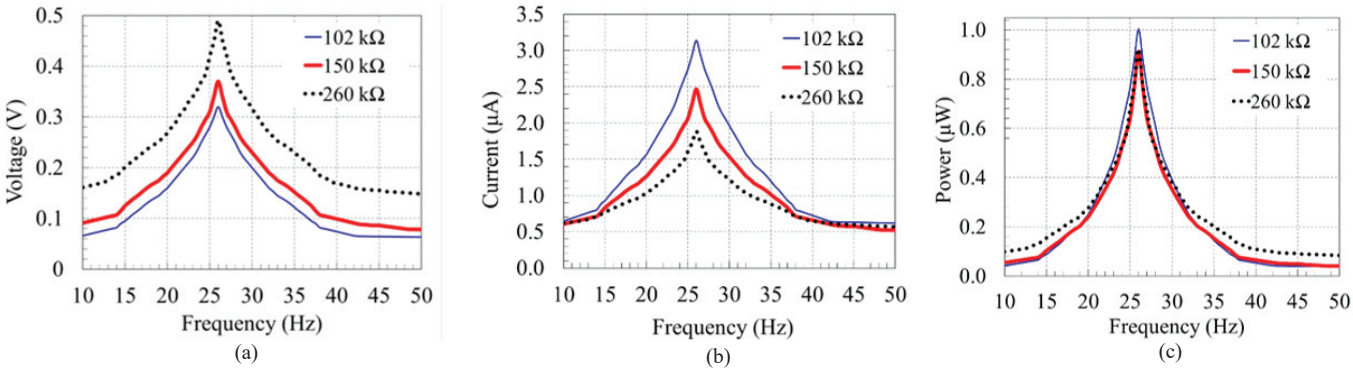

Figure 5. Predicted frequency response of harvested energy for different load resistances under harmonic excitation: (a) Voltage output, (b) Current output, and (c) Power output.

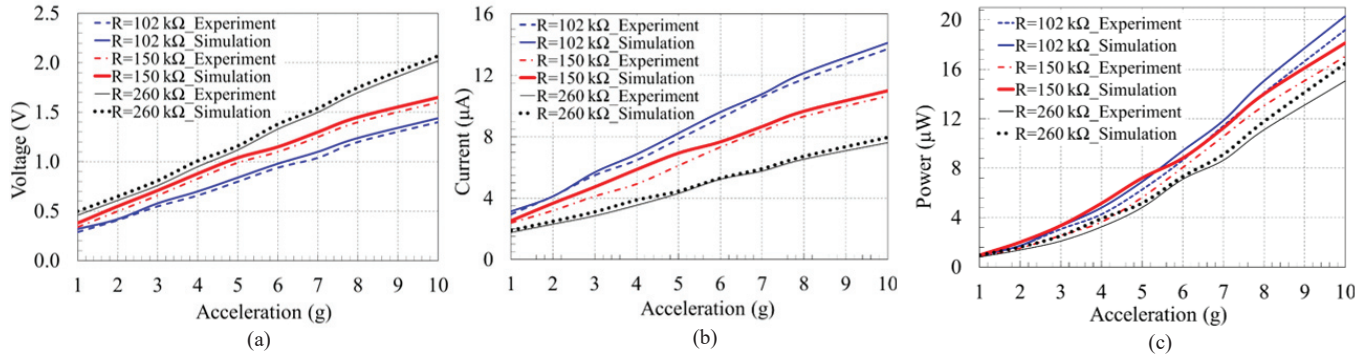

Figure 6. Effect of base acceleration on harvested energy under harmonic excitation for three different load resistances: (a) Voltage output, (b) Current output, and (c) Power (μW).

power output is from 1.04 µW to 20.4 µW, 0.93 µW to 17.70 µW and 0.93 µW to 16.5 µW, respectively at load resistance of 102 kΩ, 150 kΩ and 260 kΩ with increase in base acceleration from 1g to 10g as shown in Fig. 6(c).

3. EXPERIMENTS ON CEH UNDER HARMONIC EXCITATION

The CEH is experimented by subjecting its base to a harmonic excitation with increasing levels of accelerations, individually at three different load resistances of 102 kΩ, 150 kΩ and 260 kΩ.

3.1 Experimental Setup

The experimental setup is established as per the block diagram shown in Fig. 7(a). Actual experimental setup is shown in Fig. 7(b) and the details of CEH mounted over the vibration Shaker is shown in Fig. 7(c). An accelerometer is mounted over the Shaker for controlling the input excitations in closed loop. The apparatus employed in experimental set up is briefly described here.

Shaker and controller: The vibration shaker used for imparting the base structure's vibrational excitation is electrodynamic type with inbuilt controller having a capacity of 22.2 kN whose make: LDS, and model: V850-440SPA32K.

Energy harvester: The energy harvester is a cantilever type. The piezo-electric material is PVDF of 40 µm thickness bonded over an AA 2014 beam of 171 mm x 22 mm x 2 mm dimensions. The geometry and material properties of this CEH are as explained in Sec-3.1.

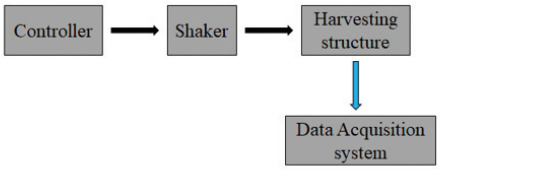

(a)

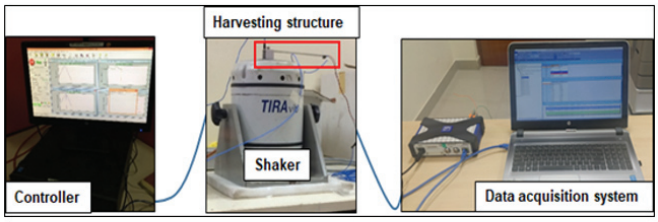

(b)

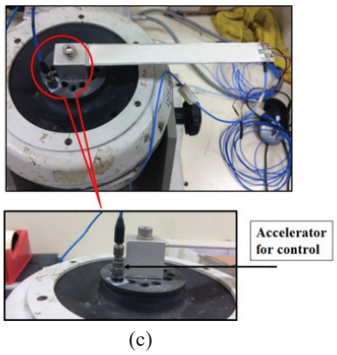

(c)

Figure 7. Experimental setup: (a) Block diagram of experimental setup, (b) Actual experimental setup, and (c) Energy harvester mounted over shaker with an accelerometer for control.

Data acquisition system (DAS): The DAS is HBM make with MX1601B model. This is used to measure and record the voltages across the load resistances when the energy harvester is excited on the Shaker.

Two resistors R_a and R_b are connected in series to facilitate the measurement of voltages V_1 and V_2 as shown in Fig. 8. In the present experimental setup, $R_a = R_b$. Two channels in DAS are used for the measurement of voltages. V_1 gives the voltage generated across the total load ($R = 2R_a$) and V_2 gives the voltage across the single resistor (R_a) for calculation of current and power.

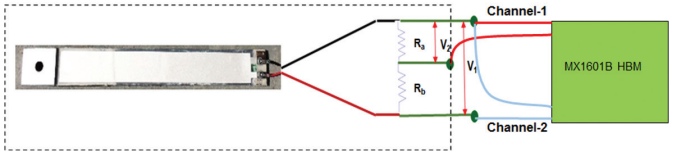

Figure 8. Experimental measurement setup for harvested voltage.

3.2 Experiments

The experiments were carried out in two stages under harmonic excitations to validate the corresponding numerical simulations. In the first stage, CEH was subjected to a harmonic base structural excitation at the fixed end with an acceleration level of 1g at a frequency varying from 10 Hz to 50 Hz with a load resistance of 102 kΩ. The fundamental natural frequency of 26.5 Hz was obtained for the CEH from the measured frequency response. In the second stage, experiments were carried out by exciting the base of CEH harmonically at natural frequency with different acceleration levels varying from 1g to 10g with load resistance as 102 kΩ. This was repeated with two more additional load resistances of 150 kΩ and 260 kΩ to experimentally investigate the harvested energy at increasing acceleration levels and increasing load resistances.

3.2.1 Harmonic Excitation at 1g with A Load Resistance

The CEH was mounted over the vibration table on top of the Shaker. The vibration table acts as a base structure for the CEH. An accelerometer was additionally mounted on top of the vibration table away from CEH as shown in Fig. 7(c). This was mounted to feedback and control the achieved vibration level in a closed loop control system. The terminals of PVDF on unimorph CEH were connected to the two equal load resistors of R_a = 51 kΩ and then to the DAS as shown in Fig. 8, which in turn was connected to the Computer. At 1g level of acceleration, the Shaker was programmed and provided a harmonic excitation to the vibration table starting from 10 Hz until 50 Hz. This range was finalised based on predicted fundamental natural frequency from numerical simulations, discussed in Sec-2.3. This frequency range covered the base excitation of approximately ±20 Hz with respect to the natural frequency of 27.5 Hz of the CEH. The voltage generated in

CEH across the two channels V_1 and V_2 were recorded. From the recorded voltages, the current I, was calculated through Ohm's law as $I=V_2/R_a$. The power P was calculated as $P=I^2R$. The voltages, current and power harvested from CEH are plotted in Figs. 4(a-b).

3.2.2 Harmonic Excitations from 1g-10g with Three Different Load Resistances

The results of aforementioned simulations and experiments have shown that the harvested energy is maximum when the base excitation matches the natural frequency of the CEH. Therefore, the experiments were carried out by exciting the base structure of CEH harmonically at 27.5 Hz i.e. at natural frequency with different acceleration levels varying from 1g to 10g with load resistance R = 102 kΩ. The voltages generated across two channels V_1 and V_2 were measured and recorded. Similar to the procedure mentioned in Sec-3.2.1, the current and power generated from each acceleration level of excitation were computed. This experiment was repeated with two more additional load resistances of 150 kΩ and 260 kΩ individually to experimentally investigate the harvested energy at increasing acceleration levels and increasing load resistances. The voltage, current and power harvested from CEH under increasing acceleration levels from 1g to 10g for three load resistances 102 kΩ ($R_a = R_b$ = 51 kΩ), 150 kΩ ($R_a = R_b$ = 75 kΩ) and 260 kΩ ($R_a = R_b$ =130 kΩ) are plotted in Fig. 6(a-c). The energy harvested and its trend are closely matching with results of numerical simulation.

4. COMPARISON OF EXPERIMENTS AND SIMULATIONS UNDER HARMONIC EXCITATION

The results from numerical simulations and experiments on CEH under base structural harmonic excitation are compared here. Initially, the frequency response of CEH under harmonic excitation ranging from 10 Hz to 50 Hz at an acceleration level of 1g for a load resistance of 102 kΩ are compared in Figs. 4(a-b). Although the experimental results were closely matching with results of numerical simulations, the numerical simulations slightly over predicted the maximum responses occurred at resonance for the load resistance. Even the fundamental natural frequency of CEH including load resistors predicted from simulation is 26.5 Hz against the experimentally determined value of 27.5 Hz. This difference of 1.0 Hz in experimental value of natural frequency may be attributed to slight difference in mass of CEH due to wire terminals connecting the CEH to the DAS and mass of resistors in the circuit. Due to the same reason, there is a slight reduction in maximum harvested energy at resonance in experiments. However, it can be observed that the area under the curve of power generated from experiment and simulation shown in Fig. 4 (b) remains almost same which represents that the energy harvested is same irrespective of the above said differences between experiment and simulation in terms of maximum harvested energy and natural frequency.

The comparison of energy harvested for three different load resistances under harmonic excitations at 1g are shown in Figs. 5(a-c) which show that as the load resistance increases, the harvested voltage increases with decrease in the current and generated power. However, the reduction in power generated is insignificant beyond 150 kΩ load resistance as shown in Fig. 5(c). The comparison of harvested energy under base harmonic excitations at increasing acceleration levels from 1g to 10g for three different load resistances 102 kΩ, 150 kΩ and 260 kΩ are shown in Figs. 6(a-c). All results clearly show that the harvested energy increases with increase in base acceleration levels. However, the trend in increase in voltage and reduction in generated current and power with the increase in load resistances are same as observed in 1g acceleration level shown in Figure 5. The decrease in power output with increase in load resistance is predominantly visible with increase in base acceleration levels as seen in Fig. 6(c) as compared to that in Fig. 5(c).

5. EXPERIMENT ON CEH UNDER RANDOM EXCITATION

The CEH was experimented by subjecting its base to a random excitation with frequency bandwidth ranging from 10 Hz to 100 Hz with acceleration spectral density ranging from 0.011 g^2/H_z to 0.71 g^2/H_z. The range of adopted acceleration spectral density corresponds to an increasing level of equivalent accelerations (root mean square, i.e. rms) ranging from $1g_{rms}$ to $8g_{rms}$. The frequency bandwidth is selected to cover up to at least three times the measured fundamental natural frequency of 26.5 Hz. The experimental setup, the method of measurement, recording of voltages and computation of generated current and power from recorded voltages are same as adopted in previous experiments under harmonic excitation explained in Sec-3.2.1. The experiments were conducted individually at each acceleration level ($1g_{rms}$ to $8g_{rms}$) at a load resistance of 102 kΩ. This experiment was repeated with two more additional resistances of 150 kΩ and 260 kΩ.

The results generated from random excitation are shown in Figs. 9(a-c). The energy harvested increases with the increase in the base excitation i.e. base acceleration level for any given load resistance. When the load resistance increases, the voltage and power generated increase and the current generated decreases.

6. COMPARISON OF HARVESTED ENERGY UNDER RANDOM AND HARMONIC VIBRATIONS

The experimentally harvested energy from CEH under harmonic and random vibrations (i.e. base excitations) with increase in base acceleration levels for three different load resistances are shown in Figs. 10(a-c). The range of harvested energy (voltage, current and power) with the increase in acceleration levels under both excitations for three load resistances are shown in Table 3. These comparisons clearly demonstrate that the equivalent random excitation yields higher energy output and the harvested energy increases almost parabolically with increase in base accelerations as compared to linear increase in harvested energy in the case of harmonic excitation.

The ratio of power harvested from random-to-harmonic excitations with increase in base acceleration is shown in Fig. 11 for three load resistances. This figure indicates that

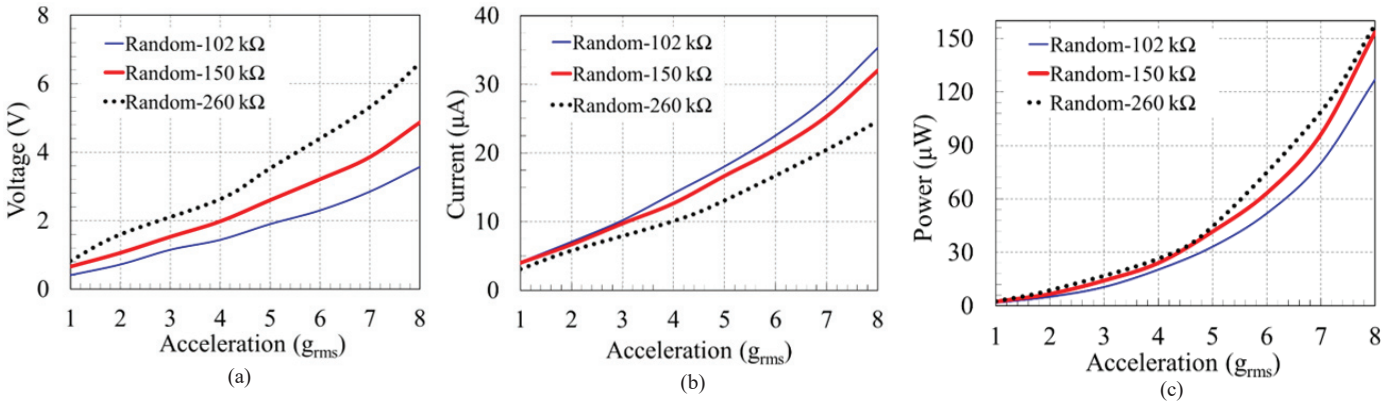

Figure 9. Effect of base acceleration on harvested energy under random excitation for three different load resistances: (a) Voltage output, (b) Current output, and (c) Power output.

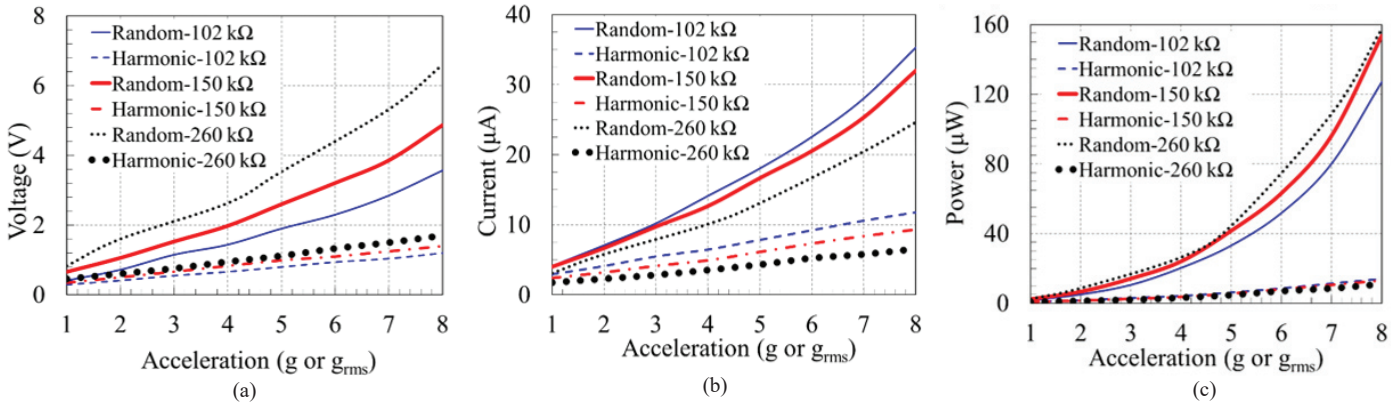

Figure 10. Harvested energy under random versus harmonic excitations for three different load resistances, under increasing base acceleration: (a) Voltage output, (b) Current output, and (c) Power output.

Table 3. Range of harvested energy under harmonic and random excitations under increasing acceleration levels from 1g to 10g from experiments

Load (kΩ)	Harmonic excitation			Random excitation		
	Voltage (V)	Current (μA)	Power (μW)	Voltage (V)	Current (μA)	Power (μW)
102	0.30 – 1.20	2.90 – 11.70	0.88 – 14.11	0.40 – 3.60	4.1 – 35.0	1.70 – 127.0
150	0.34 – 1.40	2.40 – 9.30	0.86 – 13.06	0.60 – 4.80	4.0 – 32.0	2.40 – 154.0
260	0.46 – 1.70	1.70 – 6.50	0.81 – 11.11	0.80 – 6.60	3.0 – 24.0	2.46 – 157.0

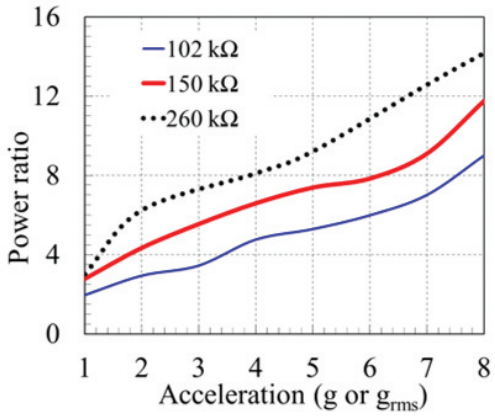

Figure 11. Ratio of harvested power between equivalent random and harmonic excitations under increasing base acceleration.

the power harvested under random excitation is 2-9 times higher for 102 kΩ, 2.8-11.8 times higher for 150 kΩ and 3-14 times higher for 260 kΩ as compared to power harvested under equivalent harmonic excitations. This demonstrate that maximum energy can be harvested when CEH is employed on base structures undergoing random vibrations as in the case of aerospace vehicles. The summary of voltage, current and power harvested from CEH under harmonic and random excitations with increasing load resistances and base accelerations is quantitatively provided in Table 3 and qualitatively in Table 4. It can be observed here that the voltage and current variations with respect to both increase in base random excitations from $1g_{rms}$ to $8g_{rms}$ and increase in load resistances are similar to that of the harmonic base excitations. But the power generated increases with increase load resistance unlike the behaviour under harmonic excitations. But, the magnitude of harvested

Table 4. Qualitative summary of harvested energy under harmonic and random excitations

Parameter	Variation with load resistance		Variation with acceleration level	
	Harmonic	Random	Harmonic	Random
Voltage	Increases	Increases	Increases	Increases
Current	Decreases	Decreases	Increases	Increases
Power	Decreases	Increases	Increases	Increases

energy under random excitation are relatively high compared to equivalent harmonic excitations.

7. CONCLUSIONS

This paper investigated the cantilever energy harvester made of PVDF and aluminium in unimorph configuration. The amount of energy harvested under random excitation as compared to equivalent harmonic excitations is clarified here which was not well understood in literature. This research highlighted the development of numerical simulation and experimental procedure and quantified the energy harvested under harmonic excitations through simulations and experiments under increasing base accelerations (1g to 10g) for three different load resistances 102 kΩ, 150 kΩ and 260 kΩ. Experimental results agreed well with simulations. Subsequently, the relative performance of this energy harvester was experimentally studied under equivalent random excitations. The following important conclusions can be drawn from the paper.

- The harvested energy is maximum when the base excitation matches the natural frequency of the harvester.
- The harvested energy increases with increase in base accelerations irrespective of the type of excitation.
- Under increasing load resistance at any given base acceleration, the harvested voltage increases and the current and power decrease in the case of harmonic excitation, whereas the harvested voltage and power increase and the current decreases in the case of random excitation.
- The decrease in power harvested with increase in load resistance under harmonic excitation is predominantly distinguishable with increasing base acceleration.
- The increase in power harvested is 2-14 times higher in random excitations as compared to equivalent harmonic excitations, with increase in equivalent base accelerations ranging from 1g to 8g for three different loads adopted in experiments.
- This cantilever energy harvester is recommended to be used in aerospace structures where random vibration amplitude is higher, to harvest more energy.

REFERENCES

1. Roundy, S.; Wright, P. K. & Rabaey, J. A study of low-level vibrations as a power source for wireless sensor nodes. *Computer Communications, 2*003, **26***,* 1131–1144. doi: 10.1016/S0140-3664(02)00248-7
2. Beeby, S. P.; Tudor, M. J. & White, N. M. Energy harvesting vibration sources for microsystems applications. *Measurement Sci. Technol.*, 2006, **17**, R175–R195. doi: 10.1088/0957-0233/17/12/R01
3. Priya, S. Advances in energy harvesting using low profile piezoelectric transducers. *J. of Electroceramics,* 2007, **19**, 167–184. doi: 10.1007/s10832-007-9043-4
4. Anton, S. R. & Sodano, H. A. A review of power harvesting using piezoelectric materials (2003–2006). *Smart Mat. Struct*., 2007, **16**(3). doi: 10.1088/0964-1726/16/3/R01
5. Cook, C. K. A.; Thambi, N. & Sastry, A. M. Powering MEMS portable devices— a review of non-regenerative & regenerative power supply systems with special emphasis on piezoelectric energy harvesting systems. *Smart Mat. Struct*., 2008, **17**(04), 3001. doi: 10.1088/0964-1726/17/4/043001.
6. Hudak, N. S. & Amatucci, G. G. Small-scale energy harvesting through thermoelectric, vibration, & radiofrequency power conversion. *J. Appl. Phys*., 2008, **103**, 101301. doi: 10.1063/1.2918987
7. Amirtharajah, R. & Chandrakasan, A. P. Self-powered signal processing using vibration- based power generation. *IEEE J. Solid-State Circuits*, 1998, **33**, 687–95. doi: 10.1109/4.668982
8. Mitcheson, P. D. MEMS electrostatic micro power generator for low frequency Operation. *Sensors Actuators A: Physical*, 2004, **115**, 523–529. doi: 10.1016/j.sna.2004.04.026
9. Dutoit N. E.; Wardle, B. L. & Kim, S. G. Design considerations for MEMS-scale piezoelectric mechanical vibration energy harvesters. *Integrated Ferroelectrics,* 2005, **71**, 121–160. doi: 10.1080/10584580590964574
10. Wang, L. & Yuan, F. G. Vibration energy harvesting by magnetostrictive material. *Smart Mat. Struct.*, 2008, **17**(4), 5009. doi: 10.1088/0964-1726/17/4/045009
11. Erturk, A. & Inman, D. J. An experimentally validated bimorph cantilever model for piezoelectric energy harvesting from base excitations. *Smart Mat. Struct*., 2009, **18**(02), 5009. doi: 10.1088/0964-1726/18/2/025009
12. Mann, B. P. & Sims, N. D. Energy harvesting from the nonlinear oscillations of magnetic levitation. *J. Sound Vibrations,* 2009, **319**(1-2), 515–530. doi: 10.1016/j.jsv.2008.06.011
13. Stanton, S. C. Nonlinear piezoelectricity in electroelastic energy harvesters: modeling & experimental identification. *J. Appl. Phys*., 2010, **108**, 074903. doi: 10.1063/1.3486519
14. Friswell, M. I. & Adhikari, S. Sensor shape design for piezoelectric cantilever beams to harvest vibration energy. *J. Appl. Phys*., 2010, **108**, 014901. doi: 10.1063/1.3457330
15. Bai, X.; Wen, Y.; Yang, J.; Li, P.; Qiu, J. & Zhu, Y. A magneto-electric energy harvester with the magnetic coupling to enhance the output performance. *J. Appl.*

Phys., 2012, **111**, 07A938.
doi: 10.1063/1.3677877

16. Aureli, M.; Prince, C.; Porfiri, M. & Peterson, S.D. Energy harvesting from base excitation of ionic polymer metal composites in fluid environments. *Smart Mat. & Struct.*, 2010, **19**(1), 5003.
doi: 10.1088/0964-1726/19/1/015003
17. Abdelkefi, A.; Nayfeh, A.H.; Hajj, M. R. & Najar, F. Energy harvesting from a multi-frequency response of a tuned bending–torsion system. *Smart Mat. & Struct*., 2012, **21**(7), 5029.
doi: 10.1088/0964-1726/21/7/075029
18. Liu, H.; Quian, Y. & Lee, C. A multi-frequency vibration-based MEMS electromagnetic energy harvesting device. *Sensors Actuators A: Physical*, 2013, **204**, 37-43.
doi: 10.1016/j.sna.2013.09.015
19. Ashraf, K.; Khir, M. M. & Dennis, J. Improved energy harvesting from low Frequency vibrations by resonance amplification at multiple frequencies. *Sensors Actuators A: Physical*, 2013, **195**, 123-32.
doi: 10.1016/j.sna.2013.03.026
20. Nechibvute, A.; Albert, C. & Pearson, L. Design & characterisation of a piezoelectric bimorph energy harvesting device. *Int. J. Eng. Tech*., 2013, **3**(6), 608-614.
21. Yu, H.; Zhou, J.; Deng, L. & Wen, Z. A vibration-based MEMS piezoelectric energy harvester & power conditioning circuit. *Sensors*, 2014, **14**, 3323-3341.
doi: 10.3390/s140203323
22. Xu, T. B. Energy harvesting from piezoelectric materials in aerospace structures. *Structural Health Monitoring in Aerospace Structures*, 2016, 175-212.
doi: 10.1016/B978-0-08-100148-6.00007-X
23. Tuma, C. & Phaoharuhansa, D. Vibration energy harvest for low frequency using double piezoelectric Cantilever beam. *In* Proceedings of International Conferences on Mechatronics and Mech Engineering, ICMME 2019, 2020, **306** 04006.
doi: 10.1051/matecconf/202030604006
24. Litak, G.; Friswell, M. I. & Adhikari, S. Magneto-piezo-elastic energy harvesting driven by random excitations. *Applied Phy. Letters,* 2010, **96**, 214103.
doi: 10.1063/1.3436553
25. Kim, M.; Hoegen, M.; John, D. & Brian, L. W. Modeling & experimental verification of proof mass effects on vibration energy harvester performance. *Smart Mat. Struct*., 2010, **19**(4), 5023.
doi: 10.1088/0964-1726/19/4/045023
26. Leng, Y.; Tan, D.; Liu, J.; Zhang, Y. & Fan, S. Magnetic force analysis & performance of a tri-stable piezoelectric energy harvester under random excitation. *J. Sound Vibration*, 2017, **406**, 146-160.
doi: 10.1016/j.jsv.2017.06.020
27. Erturk, A. & Inman, D. J. Issues in mathematical modeling of piezoelectric energy harvesters. *Smart Mat. Struct*., 2008, **17**(6), 5016.
doi: 10.1088/0964-1726/17/6/065016
28. Soliman, M.S. M.; Rahman, A.E.M.; El-Saadany, E.F. & Mansour, R.R.A wideband vibration-based energy harvester. *J. Micromech Microeng*, 2008, **18**(11), 5021.
doi: 10.1088/0960-1317/18/11/115021
29. Liu, F.; Phipps, A.; Horowitz, S.; Ngo, K.; Cattafesta, L.; Nishida, T. & Sheplak, M. Acoustic energy harvesting using an electromechanical Helmholtz resonator. *J. Acoustics Society Am.*, 2008, **123**, 1983.
doi: 10.1121/1.2839000
30. Gibus, D.; Gasnier, P.; Morel,A.; Boisseau, S. & Badel, A. Modelling and design of highly coupled piezoelectric energy harvesters for broadband applications. *J. Physics: Conference Series*, 2019, **1407** 012009.
doi:10.1088/1742-6596/1407/1/ 012009
31. Shu, Y. C. & Lien, I. C. Efficiency of energy conversion for a piezoelectric power harvesting system. *J. Micromech Microeng*, 2006, **16**(11), 2429.
doi: 10.1088/0960-1317/16/11/026
32. Shu, Y. C. & Lien, I. C. Analysis of power output for piezoelectric energy harvesting Systems. *Smart Mat. Struct*., 2006, **15,** 1499.
doi: 10.1088/0964-1726/15/6/001.
33. Shu, Y. C. & Lien, I. C. & Wu, W. J. An improved analysis of the SSHI interface in piezoelectric energy harvesting. *Smart Mat. Struct*., 2007, **16**(6), 2253–2264.
doi: 10.1088/0964-1726/16/6/028
34. Ng, T. & Liao, W. Sensitivity analysis & energy harvesting for a self-powered piezoelectric sensor. *J. Intel. Mater. Syst. Struct*., 2005, **16**, 785–797.
doi: 10.1177/1045389X05053151
35. Roundy, S. On the effectiveness of vibration-based energy harvesting. *J. Intel. Mat. Syst. Struct.*, 2005, **16**, 809–823.
doi: 10.1177/1045389X05054042
36. Renno, J. M.; Daqaq, M. F. & Inman, D. J. On the optimal energy harvesting from a vibration source. *J. Sound Vib*., 2009, **320**(1-2), 386–405.
doi: 10.1016/j.jsv.2008.07.029
37. Erturk, A. & Inman, D. J. Parameter identification & optimization in piezoelectric energy harvesting: analytical relations, asymptotic analyses, & experimental validations. *J. Syst. Control Eng.*, 2011, **225**(4), 485–496.
doi: 10.1177/0959651810396280
38. Stanton, S. C.; Owens, B .A. M. & Mann, B. P. Harmonic balance analysis of the bistable piezoelectric inertial generator. *J. Sound Vib*., 2012, **331**(15), 3617–3627.
doi: 10.1016/j.jsv.2012.03.012
39. Lefeuvre, E.; Badel, A.; Richard, C. & Guyomar, D. Energy harvesting using piezoelectric materials: case of random vibrations. *J. Electroceramics*, 2007,**19**(4), 349–355.
doi: 10.1007/s10832-007-9051-4
40. Halvorsen, E. Energy harvesters driven by broadband random vibrations. *J. Microelectromechanical Sys.*, 2008, **17**(5), 1061-1071.
doi: 10.1109/JMEMS.2008.928709
41. Adhikari, S.; Friswell, M. I. & Inman, D. J. Piezoelectric energy harvesting from broadband random vibrations. *Smart Mat. Struct.*, 2009, **18 (**11), 5005.

doi: 10.1088/0964-1726/18/11/115005
42. Marano, G.C.; Quaranta, G.; Trentadue, F;, Leqia, He & Acciani,G. Optimal design of energy harvesting from vibration subject to stochastic colored Gaussian process. *J. Phys. Commun.*, 2019, **3** 025008. doi: 10.1088/2399-6528/aad494
43. Quaranta, G.; Trentadue, F.; Maruccio, C. & Marano, G.C. Analysis of piezoelectric energy harvester under modulated and filtered white Gaussian noise. *Mech Sys. Signal Processing*, 2018, **104** 134–144. doi: 10.1016/j.ymssp.2017.10.031
44. *ANSYS Workbench User's Manual*. Version 18.1. ANSYS Corporation Inc., USA. 2019.

ACKNOWLEDGEMENTS

The authors thankfully acknowledge the support extended by Power Supplies and Instrumentation teams at Research Centre Imarat for providing the PVDF material and in preparing the unimorph specimen, and M/s. Navanidhi Electronics, Hyderabad, for providing the experimental facilities.

CONTRIBUTORS

Mr Kattamanchi Manoj has completed B.Tech in Mechanical Engineering from JNTU, Hyderabad and M.Tech in Applied Mechanics from Indian Institute of Technology Madras. He is currently pursuing PhD at NIT Warangal, in the area of energy harvesting.
He has carried out the entire FEA simulations and experiments on cantilever energy harvester reported in this paper.

Dr Vijayabaskar Narayanamurthy is currently working as Scientist-F at Research Centre Imarat, Hyderabad. His research interests include modelling of hybrid structural members, impact mechanics, flight interface structures and mechanisms.
He has primarily guided the present research work.

Dr Srikanth Korla has a PhD in Mechanical Engineering from Florida International University. He is currently serving as an Associate Professor in Mechanical Engineering at NIT Warangal. He teaches courses on solid mechanics, product design, energy harvesting, and computational techniques.
He has guided the research work on formulation of the problem.